

# Spectroelectrochemical Examination of the Interaction between Bacterial Cells and Gold Electrodes

Juan Pablo Busalmen,\* Antonio Berná, and Juan Miguel Feliu

*Instituto de Electroquímica, Universidad de Alicante, Apartado de Correos 99, 03080 Alicante, Spain*

*Received February 12, 2007. In Final Form: March 15, 2007*

The interaction between bacterial cells of *Pseudomonas fluorescens* (ATCC 17552) and gold electrodes was analyzed by cyclic voltammetry (CV) and attenuated total reflection–surface-enhanced infrared absorption spectroscopy (ATR–SEIRAS). The voltammetric evaluation of cell adsorption showed a decrease in the double-layer capacitance of polyoriented single-crystal gold electrodes with cell adhesion. As followed by IR spectroscopy in the ATR configuration, the adsorption of bacterial cells onto thin-film gold electrodes was mainly indicated by the increase in intensity with time of amide I and amide II protein-related bands at 1664 and 1549  $\text{cm}^{-1}$ , respectively. Bands at 1448 and 2900  $\text{cm}^{-1}$  corresponding to the scissoring and the stretching bands of  $\text{CH}_2$  were also detected, together with a minor peak at 1407  $\text{cm}^{-1}$  due to the  $\nu_s$   $\text{COO}^-$  stretching. Weak signals at 1237  $\text{cm}^{-1}$  were due to amide III, and a broad band between 1100 and 1200  $\text{cm}^{-1}$  indicated the presence of alcohol groups. Bacteria were found to displace water molecules and anions coadsorbed on the surface in order to interact with the electrode intimately. This fact was evidenced in the SEIRAS spectra by the negative features appearing at 3450 and 3575  $\text{cm}^{-1}$ , corresponding to interfacial water directly interacting with the electrode and water associated with chloride ions adsorbed on the electrode, respectively. Experiments in deuterated water confirmed these assignments and allowed a better estimation of amide absorption bands. In CV experiments, an oxidation process was observed at potentials higher than 0.4 V that was dependent on the exposure time of electrodes in concentrated bacterial suspensions. Adsorbed bacterial cells were found to get closer to the gold surface during oxidation, as indicated by the concomitant increment in the main IR bacterial signals including amide I, a sharp band at 1240  $\text{cm}^{-1}$ , and a broad one at 1120  $\text{cm}^{-1}$  related to phosphate groups in the bacterial membranes. It is proposed to be due to the oxidation of lipopolysaccharides on the outermost bacterial surface.

## Introduction

Bacteria growing at metal/electrolyte interfaces in the environment are exposed to the open circuit potential difference between the metal and the surrounding liquid. Because of the short decaying distance of the potential, strong electric fields are produced within the electrical double layer. It has been shown<sup>1</sup> that this can affect bacterial behavior and growth even at low polarization potentials such as those found at natural interfaces.

On approaching to a surface, the adhesion behavior of a bacterial cell is dictated by nonspecific variables as the relative charge and hydrophobicity of the interacting surfaces (i.e., the surface and the outermost bacterial layer). Also, specific interactions are known to occur that can overcome the sometimes unfavorable energetic balance of adhesion.<sup>2,3</sup> Polarizing a metal surface modifies its surface charge. Depending on the selected potential relative to the potential of zero charge (PZC) of the material, polarization may prevent or favor the adsorption of ionic or dipolar elements in the solution, including bacteria.<sup>1,2</sup> Indeed, the interfacial availability or demand of electrons at increasing overpotentials may facilitate the heterogeneous charge exchange with electroactive compounds in the cell surface, giving rise to the reduction or oxidation of cell components, respectively.

Direct evidence has been collected showing longer times to division, shorter lengths at division, and lower elongation rates for individual cells growing on a gold electrode polarized at 0.5 V (Ag/AgCl–NaCl 3 M),<sup>1</sup> as compared to those growing on a

negatively polarized surface. Indeed, biofilms grown showed a modified structure.<sup>1</sup>

In this report, the electrochemical activity of attached bacterial cells of *Pseudomonas fluorescens* was examined by cyclic voltammetry (CV) on single-crystal electrodes in order to verify whether the formerly reported effects on cell growth were related to a charge-transfer process during polarization. To identify the putative cell surface components that could be involved in this process, specific cell/surface interactions occurring during adhesion to the gold surface and the spectral variations during polarization were evaluated by attenuated total reflection–surface-enhanced infrared absorption spectroscopy (ATR–SEIRAS). This technique provides a unique opportunity to gain knowledge on the interface formed between the electrode surface and the adsorbed bacteria. Similarly to conventional ATR methods, the infrared beam travels through a high index of refraction Si prism (known as an internal reflection element, IRE) and is totally reflected at the Si/metal/electrolyte interface. An evanescent wave originates at the reflection point that penetrates into the solution, which is damped by the metal film, and interacts with species near the electrode. The presence of a metal thin film introduces the so-called SEIRA effect.<sup>4,5</sup> This is an enhancement of the infrared signal coming from physisorbed or chemisorbed species on the metal film as a result of the interaction with the excited electromagnetic field on the metal islands. The enhanced electromagnetic field is locally restricted to 3 to 4 nm away from the metal islands surface<sup>5,6</sup> and enhances infrared signals up to ca. 100 times as compared to what would be observed in its absence. This makes signals coming from the

\* Corresponding author. E-mail: jbusalmen@ua.es. Tel: +34 965903536. Fax: +34 965903537.

(1) Busalmen, J. P.; de Sanchez, S. R. *Appl. Environ. Microbiol.* **2005**, *71*, 6235–6240.

(2) Busalmen, J. P.; de Sanchez, S. R. *Appl. Environ. Microbiol.* **2001**, *67*, 3188–94.

(3) Busscher, H. J.; Weerkamp, A. H. *FEMS Microbiol. Lett.* **1987**, *46*, 165–173.

(4) Hartstein, A.; Kirtley, J. R.; Tsang, J. C. *Phys. Rev. Lett.* **1980**, *45*, 201–204.

(5) Osawa, M. *Bull. Chem. Soc. Jpn.* **1997**, *70*, 2861–2880.

(6) Wandlowski, T.; Ataka, K.; Pronkin, S.; Dising, D. *Electrochim. Acta* **2004**, *49*, 1233–1247.

interface predominate over solution signals. Furthermore, it has to be taken into account that, as stated by the surface selection rule,<sup>7,8</sup> only those vibrational modes with a dynamic dipole moment perpendicular to the surface are infrared-active during SEIRAS. This rule arises from the orientation of the enhanced electromagnetic field on the surface of the metal islands in the film.

The aim of this article is to characterize the behavior of *P. fluorescens* adsorbed on gold electrodes, emphasizing its adsorption and oxidation steps.

### Experimental Section

**Biological Material.** Pure cultures of *P. fluorescens* (ATCC 17552) were grown at 32 °C with continuous shaking in a rich broth containing bacteriologic peptone (0.5 g L<sup>-1</sup>) dissolved in 0.5% NaCl, pH 7. Cells were harvested from cultures after 18 h of growth (late exponential phase) by centrifugation for 10 min at 6000 rpm, washing with 0.5% NaCl (pH 7), and suspending in the same electrolyte to a final absorbance 600 nm higher than 1 after being centrifuged again.

**Electrode Construction.** The working electrodes used in voltammetric experiments were single-crystal beads obtained by fusion of a 0.5 mm  $\varnothing$  gold wire and cooled down slowly, as reported previously.<sup>9</sup> The surfaces of these beads contain all surface gold sites distributed uniformly. These beads were exposed to the solution, avoiding the immersion of the wire in such a way that only the polyoriented surface of the single crystal was under examination. This arrangement gives reproducible results representative of polycrystalline gold that can be easily compared in all laboratories and would lead to a better comparison of results than the use of other (wires, foils) gold electrode presentations. It precludes the use of single-crystal gold surfaces in detailed experiments. Prior to each experiment, the working electrodes were heated in a gas-oxygen flame and quenched in PureLab Ultra (Elga-Vivendi) water, following standard procedures used in surface electrochemistry.<sup>10</sup>

Gold thin-film electrodes were deposited by argon sputtering on a nonoriented monocrystalline silicon prism (Kristallhandel Kelpin, Germany) and used as working electrodes in spectroelectrochemical experiments. Deposition was carried out in the vacuum chamber of a MED020 coating system (BAL-TEC AG) equipped with a turbomolecular pump. Before deposition, the pressure was lowered to less than  $5 \times 10^{-5}$  mbar. Then, argon was admitted into the vacuum chamber to reach a pressure of around  $5 \times 10^{-2}$  mbar. The thin film thickness and the deposition rate were controlled with a quartz crystal microbalance. In all of the experiments, the film growth rate was  $0.085 \pm 0.001$  nm/s. The typical thickness of the gold thin films reported in this article is ca. 35 nm.

**Electrochemical Measurements.** Cyclic voltammetry (CV) was performed on the polyoriented bead electrodes in a four-electrode electrochemical cell using a  $\mu$ Autolab III potentiostat controlled by GPES software. The counter electrode was a coiled gold wire, and the reference was a Ag/AgCl–KCl saturated electrode connected to the main chamber through a Luggin. The reference was bridged in parallel to the solution through a 10  $\mu$ F solid-state capacitor using a second gold wire to filter high-frequency noise interference. The potential was scanned between  $-0.5$  and  $0.7$  V starting positively from  $-0.3$  V. The scan rate was  $0.01$  V s<sup>-1</sup>.

CVs were performed after the exposure of flame-annealed water quenched gold electrodes to the bacterial suspension during increasing time periods from 1 to 30 min. Preconditioned electrodes were washed with ultrapure water to eliminate loosely adhered bacteria, transferred to the electrochemical cell, and immersed after

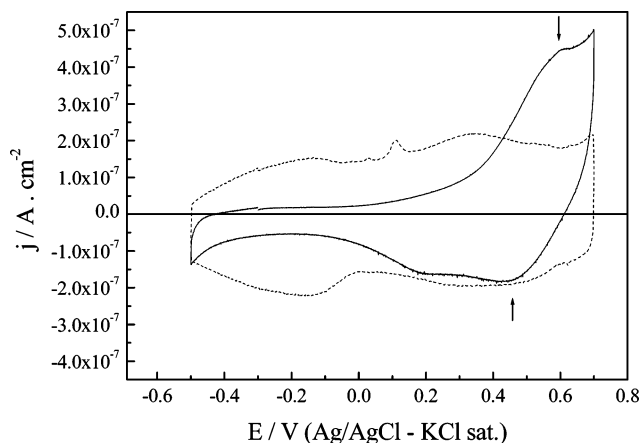


**Figure 1.** Cyclic voltammograms on a single-crystal gold electrode in 0.5% NaCl, pH 7 in the presence (—) and absence (···) of adsorbed bacterial cells. Adsorption was performed by exposing the electrode to a concentrated bacterial suspension for 10 min. Scan rate:  $0.01$  V s<sup>-1</sup>. The arrows indicate the peak position for the bacterial redox processes.

polarization at  $-0.3$  V. The electrolyte was 0.5% NaCl, pH 7. Oxygen was removed from the solution by bubbling Ar (N50, L' Air Liquide).

The time dependence of electrochemical processes of bacterial cells was determined by chronoamperometric measurements. After immersion at  $-0.3$  V, as previously indicated, the preconditioned gold electrodes were polarized at the selected potential (i.e.,  $0.7$  V), and the evolution of current was followed at  $0.1$  s time intervals for at least 200 s. All of the experiments were performed under stagnant conditions.

**ATR–SEIRAS.** Spectroelectrochemical experiments were carried out in a glass cell at room temperature (around  $20$  °C), as described elsewhere.<sup>10</sup> The cell was equipped with a prismatic  $32$  mm  $\times$   $32$  mm  $\times$   $32$  mm window beveled at  $60^\circ$  (i.e., angle of incidence =  $60^\circ$ ) and covered on one side with a gold thin film (see above). Electrical contact with the gold film was achieved through a gold foil adjusted between the gold-covered surface of the silicon prism and the glass body of the cell using a Teflon joint. A coiled gold wire and a Ag/AgCl–NaCl 3 M electrode (BAS RE-6) were used as the counter and reference electrodes, respectively. The spectrometer was a Nicolet Magna 850 equipped with a narrow-band MCT-A detector. Spectra were collected with p-polarized light with a resolution of  $8$  cm<sup>-1</sup> and are presented as the ratio  $-\log(R_2/R_1)$ , where  $R_2$  and  $R_1$  are the reflectance values corresponding to single-beam spectra at the sample and reference condition indicated in the text for each experiment, respectively. Each one of these single-beam spectra was calculated from 100 interferograms in order to reach a good signal-to-noise ratio.

After the spectra corresponding to the electrode/electrolyte interface were recorded, a concentrated bacterial suspension was added to the ATR electrochemical cell. Single-beam spectra were recorded at open circuit (around  $0.1$  V) with a 1 min time interval until no changes in the main absorption bands were observed (typically 20 min). At the end of the adsorption process, the solution in the cell was changed several times using 0.5% NaCl at pH 7 to eliminate nonadhered bacteria. Then the gold surface was loaded potentiostatically at  $0.0$  V for 2 min. It was realized that this step does not introduce any change in the single-beam spectrum taken as a reference but helps to preserve the gold film integrity during polarization. Afterward, a potential of  $0.7$  V was applied to the gold electrode. Successive 1 min elapsed spectra were recorded for an extra 10 min.

Following the procedure described above, a new series of experiments were performed using deuterated water as the solvent in order to gain insight into the influence of water on the observed IR spectra.

Conventional attenuated total reflection–Fourier transform infrared spectroscopy (ATR–FTIR) was also performed using the

(7) Nakamoto, K. *Infrared and Raman Spectra of Inorganic and Coordination Compounds*; John Wiley & Sons: New York, 1986.

(8) Socrates, G. *Infrared and Raman Characteristic Group Frequencies*; John Wiley & Sons: Chichester, U.K., 2001.

(9) Clavilier, J.; Armand, D.; Sun, S. G.; Petit, M. J. *Electroanal. Chem.* **1986**, *205*, 267–277.

(10) Berna, A.; Delgado, J. M.; Orts, J. M.; Rodes, A.; Feliu, J. M. *Langmuir* **2005**, *21*, 8809–8816.

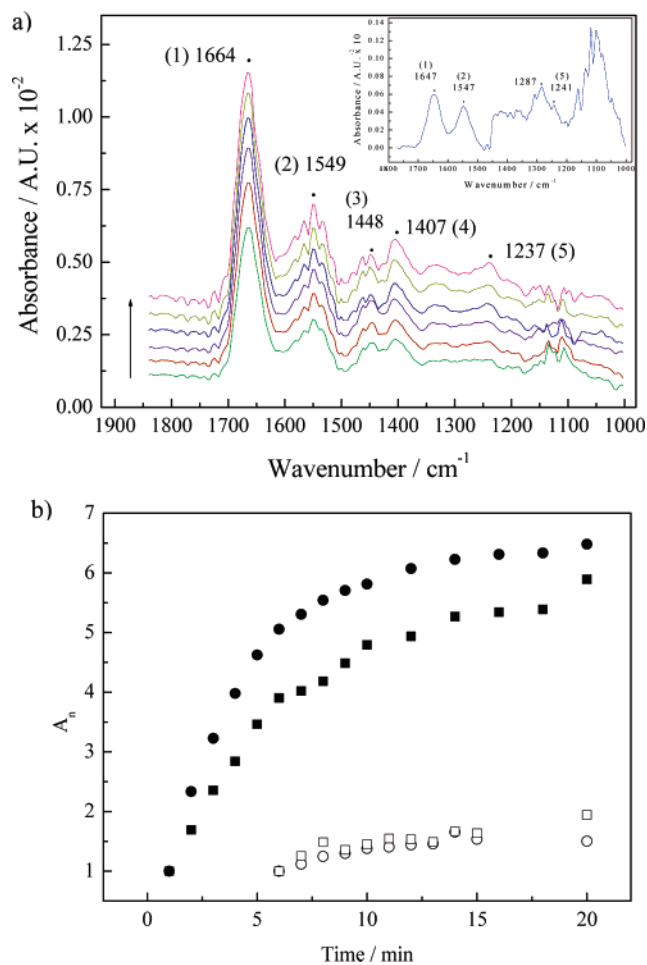


**Figure 2.** (a) Fingerprint region of ATR-SEIRAS spectra obtained after 6, 8, 10, 12, 15, and 20 min of exposure of a thin-film gold electrode to a concentrated suspension of *P. fluorescens*. The arrow indicates the direction of the time increment. (Inset) conventional ATR spectra of a concentrated suspension of *P. fluorescens* on SiO<sub>2</sub>. Approximate positions corresponding to the (1) amide I, (2) amide II, (3) CH<sub>2</sub>, (4) ν<sub>s</sub> COO<sup>-</sup>, and (5) amide III/P=O bands are indicated. Spectra were referred to that obtained in the absence of bacteria. (b) Normalized absorbance ( $A_n$ ) changes in the amide I (1664 cm<sup>-1</sup>) (circles) and amide II (1549 cm<sup>-1</sup>) (squares) bands calculated as indicated in the text from spectral data in panel a (open symbols) or from equivalent results obtained using D<sub>2</sub>O as the solvent (filled symbols).

same experimental setup as in the case of SEIRAS but in the absence of a gold deposit. This allowed the observation of the nonenhanced spectra of bacterial cells in suspension directly over the silicon prism.

## Results

**Cyclic Voltammetry of *P. fluorescens* Bacterial Cells.** A typical cyclic voltammogram obtained after exposing a poly-oriented gold electrode to a bacterial cell suspension of *P. fluorescens* is shown in Figure 1, together with results of control experiments performed in a 0.5% NaCl solution in the absence of bacteria. During control experiments, basal currents mainly arose from the charge and discharge of the double-layer capacitor. Anodic peaks at 0.0 and 0.1 V in the positive-going sweep are related to the lift of the reconstruction on the wide (111) and (100) facets present on the flame-annealed electrode surface (Figure 1).<sup>11</sup> Minor symmetric spikes at 0.6 V are due to the phase transition of adsorbed chloride

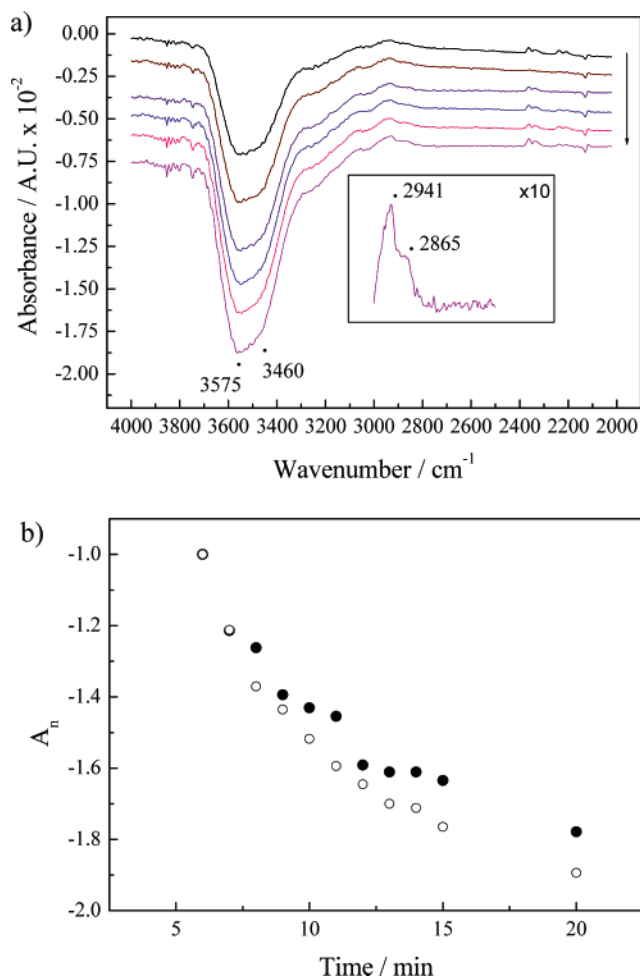


**Figure 3.** (a) High-frequency region of ATR-SEIRAS spectra obtained after 6, 8, 10, 12, 15, and 20 min of exposure of a thin-film gold electrode to a concentrated suspension of *P. fluorescens*. The arrow indicates the direction of the time increment. Approximate band positions are indicated. Spectra were referred to that obtained in the absence of bacteria. (b) Dependence on time of the normalized absorbance ( $A_n$ ) due to the water of solvation of chloride anions (3575 cm<sup>-1</sup>) (●) and interfacial bound water (3450 cm<sup>-1</sup>) (○), calculated as indicated in the text from spectral data in panel a.

anions on the wide (111) domains, which evidenced the cleanliness of the working surface and the high surface sensitivity of the CV.

The curve in the presence of adsorbed bacteria corresponds to the first voltammetric cycle obtained after contacting the solution at a potential of -0.3 V. Diminished capacitive currents in the negative potential region are due to the blocking of surface sites upon bacterial adsorption. This effect was not evident at positive potentials because of the occurrence of faradaic charge transfer. Current increases slowly at 0.1 V and more clearly beyond 0.4 V to reach a peak at around 0.6 V evidencing the oxidation of some component of the bacterial cell surface. A coupled reduction process was registered during the backward scan at a potential of 0.45 V, followed by a second, minor reduction wave with a peak potential of around 0.2 V.

**Bacterial Adsorption on Thin-Film Gold Electrodes at the Open Circuit Potential (OCP).** Results in Figure 2a show the fingerprint region of ATR-SEIRAS spectra obtained during the exposure of thin-film gold electrodes to a concentrated bacterial suspension. Major bands at 1664 and 1549 cm<sup>-1</sup> corresponding to amide I (C=O stretching) and II (N-H deformation and C-N

(11) Strbac, S.; Hamelin, A.; Adzic, R. R. *J. Electroanal. Chem.* **1993**, 362, 47-53.



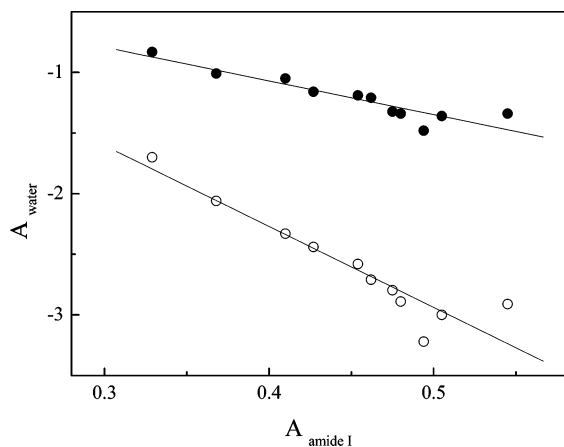


**Figure 4.** Dependence of absorbance due to both the water of solvation of chloride anions ( $3575\text{ cm}^{-1}$ ) (●) and the interfacial bound water ( $3450\text{ cm}^{-1}$ ) (○) on the amide I absorbance value.

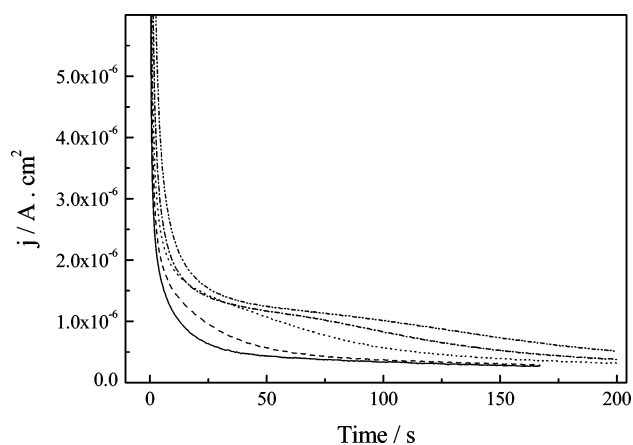


**Figure 5.** Current evolution during the polarization of single-crystal gold electrodes to  $0.7\text{ V}$  after (—) 1, (---) 2, (····) 5, (-·-·) 10, and (-·-·) 20 min of preconditioning in a concentrated bacterial suspension.

stretching) protein-related vibrations,<sup>7,8,12,13</sup> respectively, were observed to increase with time as a consequence of the progressive adsorption of bacterial cell to the electrode surface. The direct determination of the number of adhered cells on the gold surface is not possible when using the present ATR configuration, but it can be estimated from previous results<sup>2</sup> to be around  $2.5 \times 10^4$  cells  $\text{cm}^{-2}$ . Minor bands at  $1448$  and  $1407\text{ cm}^{-1}$  corresponding to the scissoring of  $\text{CH}_2$  and the  $\nu_s\text{ COO}^-$  stretching were also observed following the same increasing trend.<sup>7,8,12,13</sup> The amide III (in-phase combination of N–H in-plane bending and C–N stretching)/P=O (phospholipids) band at  $1237\text{ cm}^{-1}$  was poorly defined. Clear changes in the region between  $1100$  and  $1200\text{ cm}^{-1}$  related to the presence of alcohol groups<sup>7,8,13</sup> were regularly observed, although a dependence on time was not as evident in this last case because of the lower band intensity and the irregular baseline.

To determine the time dependence of bacterial adsorption, normalized absorbance values ( $A_n$ ) for the amide I and amide II bands were obtained by fitting the corresponding spectral region to Lorentzian functions and normalizing the values after different times  $t$  as  $A_n = A_t/A_i$ , where  $A_i$  corresponds to the initial absorbance calculated from the spectrum obtained after 6 min of exposure to the bacterial suspension. The intensity of the amide I band

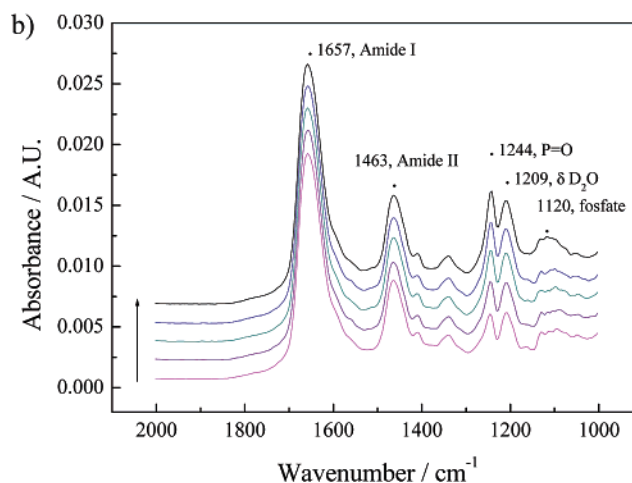
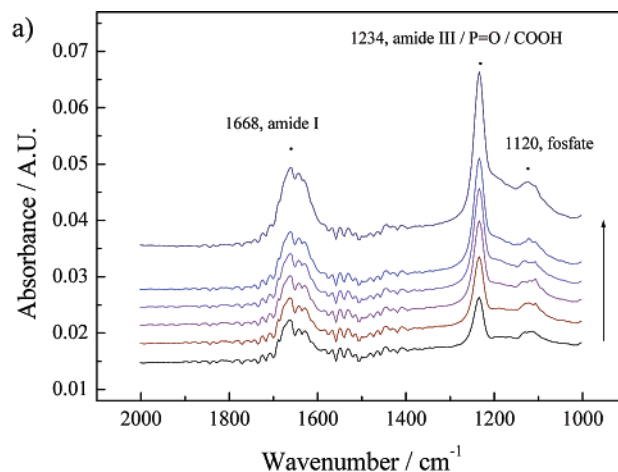


**Figure 6.** Fingerprint region of ATR–SEIRAS spectra obtained after 2, 4, 6, 8, and 10 min of polarization at  $0.7\text{ V}$  of a thin-film gold electrode for bacteria that had been adsorbed. The arrow indicates the direction of the time increment. Calculated band positions are indicated. Spectra were referred to that obtained in the absence of bacteria (a) using  $\text{H}_2\text{O}$  and (b) using  $\text{D}_2\text{O}$  as the solvent.

increased with time until reaching a saturation value after 15 min of exposure (Figure 2b). The same trend was observed in the amide II band in spite of the more dispersed data (Figure 2b). Despite the higher intensity of the amide I band, absorbance increments were slightly higher in the amide II region (Figure 2b). Additional experiments performed in  $\text{D}_2\text{O}$  solutions allowed the observation of these two bands without the interference of water. The intensity of both amide bands was found to increase, thus allowing the normalization procedure after 1 min of exposure (Figure 2b).

The adsorption of bacterial cells was accompanied by a rapid loss of interfacial water. As can be seen in Figure 3a, a deep absorbance decrease at wavelengths higher than  $3200\text{ cm}^{-1}$  indicated that the structure of coadsorbed water and double-layer anions is disrupted by the arrival of bacteria close to the surface. The disruption of the water network close to the electrode can be easily followed by the characteristic frequency of  $3460\text{ cm}^{-1}$ , corresponding to the  $\nu\text{ OH}$  stretching of interfacial water adsorbed on the electrode at potentials above the PZC.<sup>6,14</sup> The diminution of the band at  $3575\text{ cm}^{-1}$ , due to water of hydration of chloride anions<sup>15</sup> (Figure 3b), also proves the displacement of the chloride anions from the electrode surface. Water

(12) Kang, S. Y.; Bremer, P. J.; Kim, K. W.; McQuillan, A. J. *Langmuir* **2006**, *22*, 286–291.

(13) Wei, J.; Saxena, A.; Song, B.; Ward, B. B.; Beveridge, T. J.; Myneni, S. C. B. *Langmuir* **2004**, *20*, 11433–11442.

(14) Ataka, K.; Yotsuyanagi, T.; Osawa, M. *J. Phys. Chem.* **1996**, *100*, 10664–10672.

(15) Futamata, M. *Surf. Sci.* **1999**, *428*, 179–183.

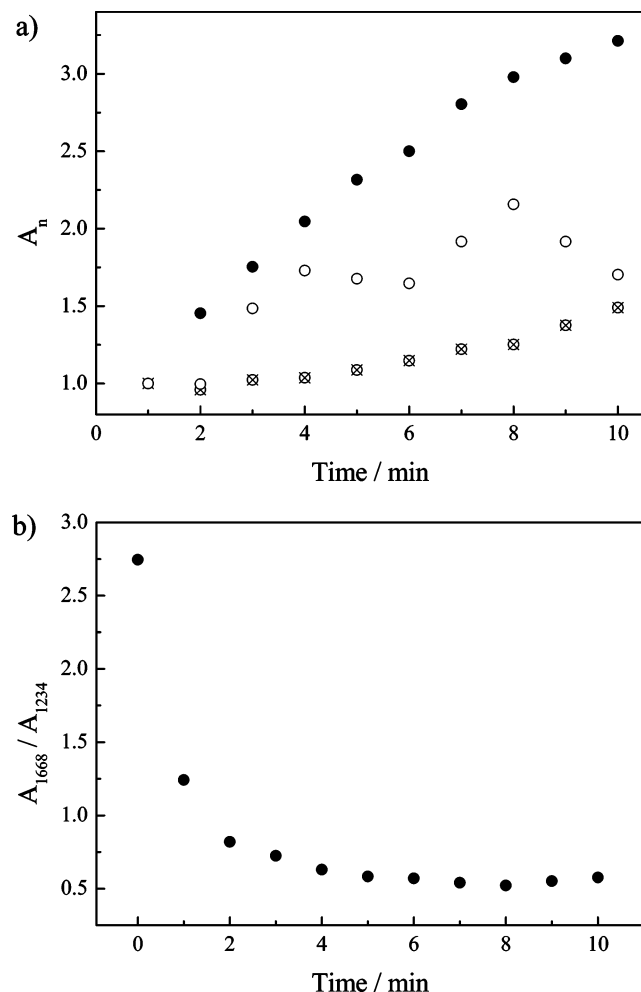


**Figure 7.** (a) Dependence on time of the normalized absorbance ( $A_n$ ) due to the amide I (⊗), amide III (●), and phosphate (○) functional groups. Values were calculated as indicated in the text from spectral data in Figure 6. The reference spectrum was taken after 1 min from the potential application. (b) Evolution of the 1668/1234 intensity ratio corresponding to values calculated as indicated in the text from spectral data in Figure 6a.

displacement follows the same kinetics as for the amide I band, as indicated by the linear proportionality shown in Figure 4. In this spectral region, two comparatively smaller positive features associated with the  $\text{CH}_2$  symmetric and asymmetric stretching vibrations appeared at 2941 and 2865  $\text{cm}^{-1}$  (Figure 3a), respectively, and were strongly perturbed by the water-related bands.

**Anodic Current from Cell Reactions.** Chronoamperometric experiments were performed to verify if the oxidation process beyond 0.6 V was related to the number of adsorbed cells and if cells were able to discharge to the electrode continuously. As can be seen in Figure 5, the current at 0.7 V was found to increase with the preconditioning time in the bacterial suspension. In all cases, after an initial spike of a few seconds the current provided by cell oxidation process rapidly decreased, showing two different decay slopes. After around 200 s, the amount of circulating current was negligible, independent of the amount of adhered bacteria (Figure 5).

**Spectral Changes in Bacteria during Polarization at 0.7 V.** Once the adsorption process at the open circuit potential reached its saturation limit (i.e., after 20 min of exposure), a potential step to 0.7 V was applied to the thin-film gold electrode in order to determine spectral changes related to the oxidation process of adsorbed bacteria.

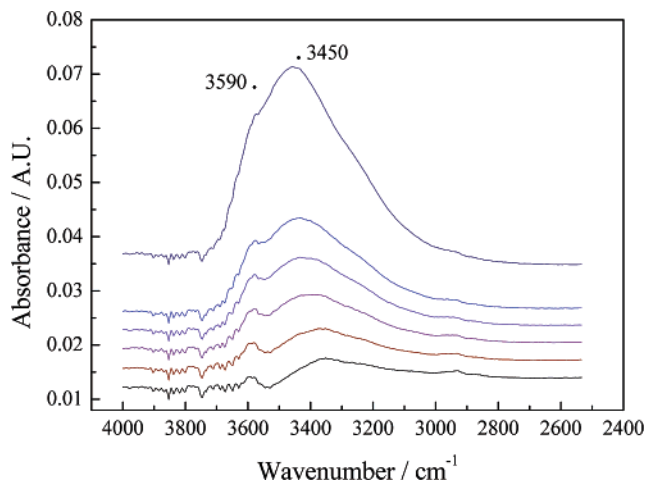


**Figure 8.** High-frequency region of ATR-SEIRAS spectra obtained after 2, 4, 6, 8, 10, and 20 min of polarization at 0.7 V of a thin-film gold electrode for bacteria that had been adsorbed. The arrow indicates the direction of the time increment. Calculated band positions are indicated. Spectra were referred to that obtained in the absence of bacteria.

Major changes were those in the bands at 1120 and 1234  $\text{cm}^{-1}$ , corresponding to phosphate and amide III/P=O/COOH, respectively (Figure 6a). Also, the amide I band at 1668  $\text{cm}^{-1}$  was observed to increase. All three bands were deconvoluted by fitting experimental data to Lorentzian functions and normalized as indicated above, in this case using the value obtained after 1 min of polarization as a reference. The corresponding intensity changes are presented in Figure 7a. A rapid increment of up to 3.5-fold in the absorbance at 1234  $\text{cm}^{-1}$  was accompanied by a 2-fold increase in that at 1120  $\text{cm}^{-1}$ . A slower increment in the signal at 1668  $\text{cm}^{-1}$  was also observed. As a consequence of these changes, the 1668/1234 ratio dropped to almost one-half of its initial value during the first minute of polarization (Figure 7b) and remained low during the rest of the experiment.

A similar but better-resolved pattern as compared to that presented in Figure 6a was observed when using deuterated water as the solvent (Figure 6b). In this case, the amide I band was slightly red shifted at 1657  $\text{cm}^{-1}$ , which could be attributed to the absence of the water band contribution, whereas the amide II band, which is more sensitive to the isotopic replacement of the hydrogen atoms, now appears at 1463  $\text{cm}^{-1}$ . The band at 1240  $\text{cm}^{-1}$  with a reduced intensity as compared to that in water was accompanied by a signal at 1209  $\text{cm}^{-1}$  corresponding to the bending mode of deuterated water.

**Water Structure Changes during Polarization in the Presence of Bacteria.** The oxidation of bacterial cells at the polarized interface was accompanied by a rearrangement of water molecules in association with the gold surface. The absorbance at 3450 and 3590  $\text{cm}^{-1}$  related to surface-associated and chloride-associated water, respectively, was observed to increase throughout the polarization step (Figure 8). It is important to note that the absorbance of reentering water is several times higher than that of displaced water in Figure 3a. Taking into account that in SEIRAS experiments the intensity is not a linear function of the distance to the surface,<sup>5</sup> the observed difference could be tentatively related to a higher enhancement of water signals due to the closer approach of water molecules to the positively charged gold surface.

## Discussion

Upon interacting with a surface, bacterial cells come under new environmental conditions that are determined by the

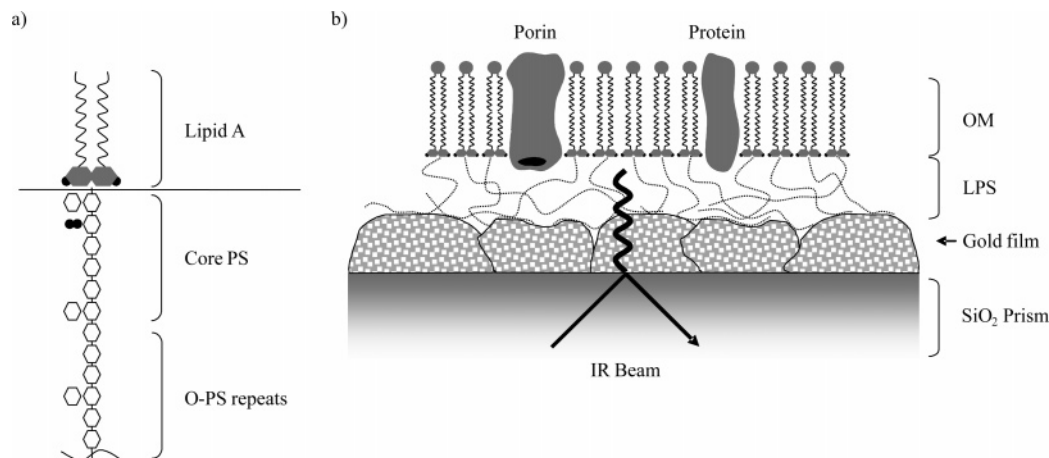


**Figure 9.** (a) Schematic representation of a typical lipopolysaccharide molecule showing Lipid A, the core polysaccharide (Core PS), and the oligopolysaccharide repeats (O-PS). (b) Graphical abstract of the bacteria/thin-film gold electrode interface in the ATR-SEIRAS configuration showing the interaction with the attenuated IR evanescent wave. OM: outer membrane; LPS: lipopolysaccharides. (●) Phosphate groups.

physicochemical features of the substratum and may influence its behavior. In particular, when adhering to a conducting surface such as that of metals, bacterial cells are often exposed to electric fields originating in the potential difference across the metal/electrolyte interface. Beside this, external polarization is often applied to structures or electrodes in contact with natural water or wastewater with a technological aim. Good examples are the use of negative polarization for the cathodic protection of metal structures<sup>16</sup> or the positive polarization of electrodes in bio-fuel-cell applications.<sup>17,18</sup>

The existence of a potential difference at a surface denotes the possibility of doing chemical or physical work. In fact, the electrostatic pulling of bacterial cells to a positively charged surface<sup>1</sup> can be seen as a manifestation of physical work, while a heterogeneous charge-transfer processes can be related to chemical work. As exerted on bacterial cells, this work can modify their behavior, trigger their metabolic response, or even determine their fate upon adhering to a surface.

To enable charge transfer, close contact is required between bacterial cells and the polarized surface. It has been previously shown<sup>2</sup> that *P. fluorescens* cells can readily adhere to a gold surface at the OCP in a neutral NaCl solution because of the attractive interaction energy determined by the positive charge of the surface. The same was observed in the present work, where the increment in the amide I and II bands (Figure 2b) showed that bacteria increasingly adhered to a thin-film gold electrode during ATR-SEIRAS experiments, reaching a stationary maximum coverage after 20 min of exposure.

**Specific Interactions between Bacteria and a Gold Thin-Film at the OCP.** The outer membrane of gram-negative cells such as those of *P. fluorescens* is known to present a typical bilayer lipid structure with embedded proteins. The major structural components of this membrane are lipopolysaccharides (LPS) composed of a hydrophobic moiety anchored to the membrane (lipid A) and hydrophilic carbohydrate domains that protrude into the surrounding liquid.<sup>19</sup> Lipid A consists of fatty acids linked to a phosphorylated disaccharide (two glucosamine residues), whereas the carbohydrate side includes an oligosac-

charide core that is usually substituted with phosphoric acid, ethanolamine, phosphoethanolamine, or acetyl groups (Figure 9). Finally there are O-specific polysaccharide chains that extend to the solution, consisting of repeated oligosaccharide units whose structure may significantly vary in different strains<sup>19</sup> (Figure 9). Within the described elements, those located at the outermost side of the bacterial envelope (i.e., the oligosaccharides ends of LPS) are the main candidates involved in the physical contact with the gold surface. This is in agreement with the detection of IR-absorbing vibrations from 1100 to 1200 cm<sup>-1</sup> in the spectra in Figure 2a, which are known to be related to the hydroxyl groups in carbohydrates.<sup>13</sup> Nevertheless, in accordance with results reported by others for *P. aeruginosa* using conventional ATR on Ge or ZnSe crystals,<sup>12,13</sup> the main features in the IR spectra obtained during the adsorption of bacteria were those related to the presence of proteins (amide I and II bands in Figure 2a).

Taking into account that the surface enhancement effect of SEIRAS is ascribed only to those molecules chemisorbed on the surface and sharply decays at distances larger than 5 nm,<sup>5</sup> the results in Figure 2a indicate that not only the LPS but also those elements located at deeper positions in the bacterial core (e.g., proteins) were in contact with the surface or within the enhanced electromagnetic field (Figure 9b).

The energies and intensities of amide bands have been found to be sensitive to conformational changes of proteins,<sup>20,21</sup> with an amide I/amide II ratio that was found to increase with changes in folding.<sup>20</sup> Interestingly, an increased ratio of 1.27–3.45 has been assigned to conformational changes during protein interaction with mineral oxides.<sup>22</sup> Typical ratios of ~1 can be observed in the amide I/amide II ratio of *Pseudomonas* cells using conventional ATR-FTIR spectroscopy (inset of Figure 2a).<sup>12,13,22</sup> In the absence of any surface enhancement effect, these values are intended to be a consequence of the overall conformational state of proteins in the membrane of bacteria located within the distance range of the ATR evanescent field. The use of SEIRAS, however, allowed the selective analysis of proteins contacting the gold surface. An amide I/amide II ratio of 2.0 ± 0.1 can be calculated from results in Figure 2a during the adsorption of cells to the gold surface (data not shown), suggesting that upon interaction with the surface, proteins are partially unfolded or

(16) Orfei, L. H.; Simison, S.; Busalmen, J. P. *Environ. Sci. Technol.* **2006**, *40*, 6473–6478.

(17) Logan, B. E.; Hamelers, B.; Rozendal, R.; Schroder, U.; Keller, J.; Freguia, S.; Aelterman, P.; Verstraete, W.; Rabaey, K. *Environ. Sci. Technol.* **2006**, *40*, 5181–5192.

(18) Rabaey, K.; Verstraete, W. *Trends Biotechnol.* **2005**, *23*, 291.

(19) Veremeichenko, S. N.; Vodyanik, M. A.; Zdorovenko, G. M. *Appl. Biochem. Microbiol.* **2005**, *41*, 365–371.

(20) Ishida, K. P.; Griffiths, P. R. *Appl. Spectrosc.* **1993**, *47*, 584–589.

(21) Buijs, J.; Norde, W.; Lichtenbelt, J. W. T. *Langmuir* **1996**, *12*, 1605–1613.

(22) Parikh, S. J.; Chorover, J. *Geomicrobiol. J.* **2005**, *22*, 207–218.



denatured.<sup>20</sup> Indeed, a shift in the position of the amide I peak from the reference value of 1647  $\text{cm}^{-1}$  (inset of Figure 2a) or those even lower reported by others<sup>22</sup> to an actual value of 1664  $\text{cm}^{-1}$  (Figure 2a) may signal some degree of conformational change to an unordered state<sup>21</sup> within proteins contacting the surface.

The low intensity of the amide III/P=O/COOH band at 1237  $\text{cm}^{-1}$  and the absence of the band at 1080  $\text{cm}^{-1}$  due to alcoholic OH in the LPS as compared to those results obtained by conventional ATR (inset of Figure 2a)<sup>12,13</sup> are also indicative of the surface selectivity of spectra in Figure 2a.

The direct physical contact between bacteria and the gold surface requires the displacement of water. The presence of bacteria at the interface strongly affects the network of water and anions coadsorbed on the surface of the electrode. Negative bands in the ATR–SEIRAS spectra provide information about the structure of water on the surface before bacteria were added and indirectly about how closely bacteria are approaching the electrode surface. Bands at 3460 and 3575  $\text{cm}^{-1}$  are due to water molecules adsorbed on the surface. The latter band is due to the water of hydration of chloride anions adsorbed on the surface,<sup>15</sup> and the former band comes from water molecules oriented with the two hydrogen atoms toward the solution and interacting with the electrode surface through the oxygen lone-pair electrons.<sup>14</sup> This picture matches the state of water coadsorbed with anions that do not facilitate hydrogen bonding on gold electrodes at potentials higher than the potential of zero charge,<sup>6,14,15</sup> confirming that the surface bears a net positive charge at the open circuit potential under the actual experimental conditions,<sup>1,2</sup> which is known to favor the adsorption of bacteria. The substitution of the water/anion network by bacteria evidences its more favorable interaction with the electrode surface.

Besides the features at high frequencies presented in Figure 3, a decreasing trend in the absorption at 1650  $\text{cm}^{-1}$  should be observed as a result of the bending vibration of displaced water, thus influencing the changes observed in the amide I band in Figure 2. To gain insight into this effect, experiments were repeated using deuterated water as the solvent. Preliminary results showing the increment of a much more intense amide I band in Figure 2b reinforce the conclusion about protein unfolding upon interaction with the gold surface.

#### Bacteria–Gold Surface Interactions during Polarization.

Changes due to the adsorption of bacteria modified the electrochemical response of the interface. The replacement of ions and water at the electrical double layer of gold strongly blocked the surface, thus diminishing capacitive currents (Figure 1). At positive potentials, although still unidentified, the oxidation of some cellular component was evident (Figure 1). The amount of charge transferred at 0.7 V was consistently observed to decrease in consecutive CV cycles (data not shown), evidencing some irreversibility in the oxidative process. When comparing currents obtained after increasing preconditioning times, an increasing trend was observed showing a direct relation with the number of adsorbed cells (Figure 5). Currents were exhausted after 200 s of polarization, suggesting a relation to the oxidation of a cell element present in a limited quantity.

Spectral changes registered under polarization during ATR–SEIRAS experiments can bring the identity of the oxidized cell elements to light. It is important to note that free-swimming bacteria were removed from the solution before applying polarization (Experimental Section), which restricts the observed changes to irreversibly adhered bacteria. Major changes in the fingerprint spectral region were the intensity increments at 1120, 1234, and 1668  $\text{cm}^{-1}$  (Figure 6), within which differences were

observed in the kinetics of increase (Figure 7). Higher values in the main IR signals of *Pseudomonas* cells with truncated LPS have been previously justified by a shorter distance within the cells and the surface.<sup>12</sup> In this direction, it is proposed that because of the strong electrostatic attraction during polarization at a positive potential, adhered bacteria are forced to get closer to the surface, thus increasing the specific contact area and the IR signals. In this context, the faster increment in the signals at 1120 and 1234  $\text{cm}^{-1}$  may involve the detection of new bacterial elements located at deeper sites in the bacterial core or may be due to the formation of an oxidation product at the applied potential (Figure 1).

Within chemical groups at the bacterial envelope, LPS are located outermost and are present in major quantities. It is speculated that the oxidation of hydroxyl groups in oligosaccharide chains of LPS can be the source of currents reported in Figures 1 and 5. This is based on the fact that one of the usual assignments of the 1234  $\text{cm}^{-1}$  frequency signal is the C–OH stretching in COOH groups. Although these groups are predominantly dissociated at neutral pH ( $\text{p}K_a$  5),<sup>23</sup> the acidification of the interface as a consequence of the electrochemical oxidation of alcohols may allowed their occurrence in the protonated state. The spectrometric detection of COOH groups as a product of LPS oxidation has also been reported during the photocatalytical inactivation of *E. coli* cells adsorbed onto  $\text{TiO}_2$  films.<sup>24</sup> Considering that oxidation currents were almost exhausted after 200 s of polarization (Figure 5), the rapid decay in the 1668/1234  $\text{cm}^{-1}$  (Figure 7b) ratio could also indicate that LPS oxidation precedes the bacterial movement toward the surface.

The detection of the band at 1120  $\text{cm}^{-1}$  (Figure 6), however, could be related to phosphate groups in the polar head of lipid A that become detectable as a result of the movement of bacterial cells toward the surface. These groups can also contribute to the increase in the 1234  $\text{cm}^{-1}$  signal. As can be seen in Figure 6b, the resolution in the region around 1200  $\text{cm}^{-1}$  was improved during the experiments performed in  $\text{D}_2\text{O}$ , which could help to determine the contributions of amide III, phosphate, and COOH absorptions in the polarization effects. The band at 1234  $\text{cm}^{-1}$  showed a reduced intensity that is thought to be due to a separation of the complex contributions found in water. The shift in the amide III and COOH bands as a result of the isotopic exchange allowed the observation of the phosphate contribution at this frequency, which together with the observation of the phosphate signal at 1120  $\text{cm}^{-1}$ <sup>7</sup> (also unaltered in  $\text{D}_2\text{O}$ ) gives support to the proposed movement of bacteria toward the surface as a consequence of polarization.

In the region beyond 3000  $\text{cm}^{-1}$ , two positive features at 3590 and 3450  $\text{cm}^{-1}$  started to grow during polarization likely as a result of the building of a coadsorbed chloride and water network on the positively charged surface (Figure 8). Different from typical double-layer processes that are very fast, the increase in the intensity of these bands expands over minutes, suggesting a relation with the oxidation process of bacterial surface elements. The accumulation of water at the interstitial space between cell bodies and the surface could be related to one or all of the following processes: (a) its formation as a product during LPS oxidation, (b) the re-entrance of some quantity of water due to the detachment of the carbohydrate ends of LPS after oxidation, and (c) the more favorable interaction of newly formed carboxylic groups with solvation water entering the interstitial space. In conjunction, all of these process would explain the intensity

(23) Martell, A. E.; Smith, R. M. *Critical Stability Constants*; Plenum Press: New York, 1977.

(24) Nadochenko, V.; Denisov, N.; Sarkisov, O.; Gumy, D.; Pulgarin, C.; Kiwi, J. *J Photochem Photobiol, A* **2006**, *181*, 401–407.

increase in the band at  $3450\text{ cm}^{-1}$ . Additionally, a change in the orientation of the water dipole moment toward a more perpendicular position with respect to the gold surface may also contribute to increase this signal. Because bacteria remain attached by the direct interaction between proteins and gold, the occurrence of a certain amount of isolated water hidden to participate in the water network can be suspected. These molecules would contribute to the band at  $3590\text{ cm}^{-1}$ .

At the end of the experiments, the potential of the gold surface was lowered to 0.0 V to evaluate the reversibility of changes observed during the polarization at 0.7 V. No relevant changes were detected under these conditions (data not shown).

The integrity of LPS is known to be important for membrane stability and cell viability.<sup>25</sup> The phosphorylation of the inner core residues is known to provide the binding sites for the establishment of divalent cation bridges between adjacent LPS molecules and plays a crucial role in the stabilization of membranes.<sup>25</sup> Defects associated with membrane instability include hypersensitivity to hydrophobic antibiotics and detergents, the release of increased amounts of periplasmic proteins, and the lack of expression of pili and flagella, among others. Some of these effects can influence cell growth and biofilm formation.<sup>25</sup> In this sense, the oxidation of LPS may be related to the previously observed effects of polarization on cell growth and biofilms.<sup>1</sup>

Because membrane stability depends on the electrostatic interaction between LPS molecules and taking into account the ATR–SEIRAS demonstration of the close contact between the outer cell membrane and the electrode, it is proposed that because of the polarization-driven oxidation of LPS molecules contacting the gold surface, structural changes are introduced into the outer membranes of cells that modify membrane functions that are relevant to growth. Similarly, the oxidation of membrane cell elements, including LPS, has been proposed as the main cause for the photokilling effect of UV light on bacteria adsorbed on the semiconductor surface of  $\text{TiO}_2$ .<sup>24</sup> Additionally, a direct effect of the electrochemical potential on the electric double layer of the outer cell membrane cannot be discarded. Taking into account the importance of electrostatic interactions in cell membrane stability, the rearrangement of counter ions as a consequence of polarization could also have a similar deleterious effect on bacterial integrity. The leaking of molecules from the periplasmic space might be suspected after outer membrane disruption, which could also play a role in the observed spectral changes.

**Acknowledgment.** Financial support from the European Union through a Marie Curie International Incoming fellowship (contract no. MIF1-CT-2006-021347) is acknowledged. Partial support from the MEC (Spain) through project CTQ2006-04071/BQU is also acknowledged.

(25) Raetz, C. R. H.; Whitfield, C. *Annu. Rev. Biochem.* **2002**, *71*, 635–700.